Gaining insight into transcriptome-wide RNA population dynamics through the chemistry of 4-thiouridine

Erin E. Duffy,

Department of Molecular Biophysics & Biochemistry, Yale University, New Haven, CT 06511, USA, Chemical Biology Institute, Yale University, West Haven, CT 06516, USA, Erin.Duffy@yale.edu

Jeremy A. Schofield,

Department of Molecular Biophysics & Biochemistry, Yale University, New Haven, CT 06511, USA, Chemical Biology Institute, Yale University, West Haven, CT 06516, USA, Jeremy.Schofield@yale.edu

Matthew D. Simon

Department of Molecular Biophysics & Biochemistry, Yale University, New Haven, CT 06511, USA, Chemical Biology Institute, Yale University, West Haven, CT 06516, USA, Matthew.Simon@yale.edu

Abstract

Cellular RNA levels are the result of a juggling act between RNA transcription, processing, and degradation. By tuning one or more of these parameters, cells can rapidly alter the available pool of transcripts in response to stimuli. While RNA sequencing (RNA-seq) is a vital method to quantify RNA levels genome-wide, it is unable to capture the dynamics of different RNA populations at steady-state or distinguish between different mechanisms that induce changes to the steady-state (i.e. altered rate of transcription versus degradation). The dynamics of different RNA populations can be studied by targeted incorporation of non-canonical nucleosides. 4-thiouridine (s^4U) is a commonly used and versatile RNA metabolic label that allows the study of many properties of RNA metabolism from synthesis to degradation. Numerous experimental strategies have been developed that leverage the power of s^4U to label newly transcribed RNA in whole cells, followed by enrichment with activated disulfides or chemistry to induce C mutations at sites of s^4U during sequencing. This review presents existing methods to study RNA population dynamics genome-wide using s^4U metabolic labeling, as well as a discussion of considerations and challenges when designing s^4U metabolic labeling experiments.

Graphical/Visual Abstract and Caption
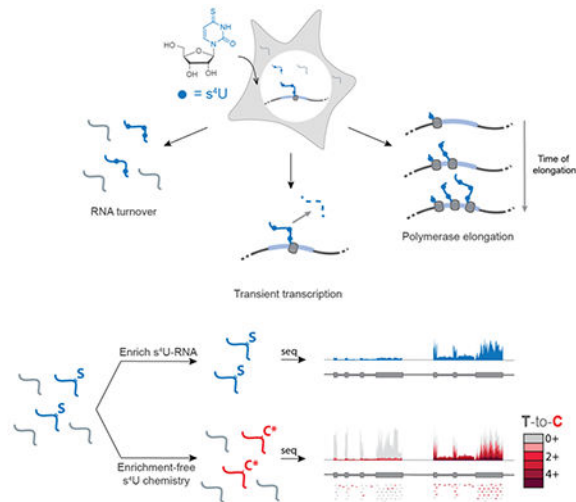
Newly transcribed RNAs can be metabolically labeled with 4-thiouridine (s^4U) to study many aspects of RNA metabolism genome-wide, including RNA turnover, transient transcription, and polymerase elongation. New RNAs can be detected via biochemical enrichment (top) or nucleoside recoding to induce U to C mutations in s^4U-RNA in high-throughput sequencing.

INTRODUCTION

RNA levels are determined by the tight regulation of RNA synthesis and degradation. Eukaryotes can modulate RNA levels by altering transcription, processing or decay. This dynamic regulation can lead to the same RNA steady-state levels via multiple pathways. For example, a cell can increase RNA levels by increasing transcription or decreasing degradation. Therefore, while RNA-seq can be used to detect changes in RNA levels upon stimulation, one cannot distinguish what mechanism led to a given RNA profile. Detailed studies of the kinetics of RNA transcription and degradation have been performed in response to a range of stimuli such as lipopolysaccharide (LPS) in mouse dendritic cells (Rabani et al., 2011), interleukin 7 (IL7) in mouse naïve T-cells (Li et al., 2017), and 4-hydroxytamoxifen (OHT) in mouse fibroblasts (de Pretis et al., 2017). These studies demonstrate that cells regulate RNA levels by multiple mechanisms in a transcript-specific manner. RNA turnover can be tissue-specific as well as stimulus-specific, highlighting the need to understand the contribution of RNA population dynamics in a variety of metabolic and cellular contexts.

Standard biochemical analyses have been widely used to probe specific aspects of RNA regulation. These include RNA polymerase II (RNAPII) ChIP and nuclear run-on to study transcription, as well as transcriptional shutoff using small molecules to study RNA degradation. However, metabolic labeling with non-canonical nucleosides provides a handle for analysis of transcripts throughout the lifetime of the RNA, creating a versatile platform to probe many facets of RNA metabolism in a single experimental workflow. This versatility not only streamlines experimental optimization, but also enables clearer interpretation of cellular responses where changes in RNA synthesis and degradation simultaneously occur.

In order to study the dynamics of different populations of RNA, classic studies used incorporation of radiolabeled orthophosphate or nucleotides that facilitated analysis of bulk RNA population dynamics (for early examples, see (Hokin & Hokin, 1954; Logan, Heagy, & Rossiter, 1955; Muramatsu & Busch, 1964). However, the application of non-canonical nucleosides opened the door for later genome-wide analyses by enabling the biochemical separation of new RNAs from pre-existing RNAs (reviewed by (Tani & Akimitsu, 2012). The three most common non-canonical nucleosides used for metabolic labeling of RNA are 5-bromouridine (BrU), 5-ethynyluridine (EU) and 4-thiouridine (s^4U) (Box 1). BrU triphosphate can be added to isolated nuclei in global nuclear run-on sequencing (GRO-seq, (Core, Waterfall, & Lis, 2008) to study transcription, or BrU nucleoside can be incorporated into whole cells to study RNA stability (BRIC-seq,(Tani et al., 2012). Both techniques enrich BrU in newly transcribed RNAs by immunoprecipitation with anti-BrdU antibodies in order to separate new RNAs from old. Alternatively, 5-ethynyluridine (5-EU) can be incorporated into newly transcribed RNAs in whole cells and enriched using click-chemistry (Jao & Salic, 2008), a strategy which was later adapted to a high-throughput sequencing platform (Meryet-Figuiere et al., 2014). Click-compatible nucleosides hold the advantage that they are orthogonal to cellular functional groups and therefore can be used for a wide variety of applications including RNA imaging (Jao & Salic, 2008) with reduced cross reactivity with other macromolecules including proteins. The use of BrUTP in nuclear run-on experiments has been replaced with the use of biotinylated nucleotide triphosphates for streptavidin purification (PRO-seq, Kwak, Fuda, Core, & Lis, 2013). These PRO-seq experiments and analogue-free enrichment strategies based on the immunopurification of RNAPII (NET-seq, (Churchman & Weissman, 2011) can reveal the 3'-most nucleotide in a nascent transcript, providing high resolution views of transcription. Finally, s^4U is rapidly incorporated into newly transcribed RNA in living cells without the need for nuclear isolation. As we will discuss in detail below, s^4U provides a range of chemical opportunities. s^4U-RNA can be enriched using activated disulfides conjugated to biotin, which hold the advantage that this chemistry is covalent (unlike BrU) and the disulfide bond is reversible (unlike EU), allowing for efficient elution of s^4U-RNA from streptavidin beads and analysis. As an alternative to biochemical enrichment, the presence of s^4U in an RNA can be identified by chemically recoding the hydrogen bonding pattern of s^4U to induce apparent T-to-C mutations in genome-wide RNA-seq experiments (Herzog et al., 2017; Schofield, Duffy, Kiefer, Sullivan, & Simon, 2018). These opportunities provide a common platform to study the kinetics and regulation of the entire RNA life-cycle from synthesis to degradation.

Historically, metabolically labeled s^4U-RNAs were isolated using organomercurial affinity matrices (Melvin, Milne, Slater, Allen, & Keir, 1978) based on the high affinity of thiols for mercury. While this purification strategy remains a powerful way to enrich s^4U-RNA (for example, see (Kenzelmann et al., 2007; Ussuf, Anikumar, & Nair, 1995; Woodford, Schlegel, & Pardee, 1988), the practicality of s^4U metabolic labeling was expanded with the development of activated disulfide purification; the endogenous uracil phosphoribosyltransferase (UPRT) activity in *T. gondii* was harnessed to metabolically label cells with 4-thiouracil and enrich RNAs using HPDP-biotin, a 2-pyridylthio-activated disulfide of biotin, followed by enrichment using a streptavidin matrix (Cleary, Meiering, Jan, Guymon, & Boothroyd, 2005). Later, s^4U nucleosides were found to be incorporated

into mammalian cells without the need for UPRT expression (Dölken et al., 2008), thereby streamlining the process of metabolic labeling and expanding the utility of this method to many different cell types.

Following the application of s^4U to metabolically label newly transcribed RNAs in mammalian cells, this strategy revealed relationships between mRNA half-lives and protein stability (Friedel, Dolken, Ruzsics, Koszinowski, & Zimmer, 2009; Schwanhäusser et al., 2011). In parallel, important s^4U metabolic labeling experiments were achieved in *S. cerevisiae* through the expression of exogenous transporters (hENT1 (C. Miller et al., 2011) or Fui1 (Swiatkowska et al., 2012) that are necessary for efficient s^4U uptake and RNA labeling (unlike *S. pombe* that express UPRT or mammalian cells that express uridine transporters). Following these single time point analyses, multiple time point experiments were developed in yeast, including a pulse-chase approach to reveal RNA stability and a time course of s^4U labeling to study RNA processing and/or stability (Munchel, Shultzaberger, Takizawa, & Weis, 2011; Neymotin, Athanasiadou, & Gresham, 2014; Windhanger et al., 2012). Transient RNAs, including introns and unstable non-coding RNAs, were enriched in yeast following 1.5 to 5 min of s^4U labeling (Barrass et al., 2015), and in human cells following 5 min of s^4U labeling (Schwalb et al., 2016; Windhanger et al., 2012). These techniques illustrate the diverse array of experimental strategies that leverage s^4U metabolic labeling and allow for the study of RNA metabolism in many different cell types and biological contexts.

In addition to improvements in experimental design, methodologies for detecting s^4U-RNAs have also advanced. While HPDP-biotin expanded the use of s^4U metabolic labeling, it was later shown to be inefficient in its reactivity with s^4U, leading to low yields and biases in enrichment (Duffy et al., 2015). A more efficient activated disulfide, methane thiosulfonate conjugated to biotin (MTS-biotin), was demonstrated to improve s^4U metabolic labeling by increasing yields and alleviating length bias. This advance enabled the first study of s^4U labeled microRNA turnover in proliferating cells, which revealed a population of mature miRNAs with rapid turnover in 293T cells (Duffy et al., 2015). Recently, methane thiosulfonate was directly coupled to magnetic sepharose, which reduces the number of handling steps through a one-step capture of s^4U-RNAs (Duffy, Canzio, Maniatis, & Simon, 2018). This enables s^4U-RNA enrichment from small numbers of cells and extending the utility of s^4U metabolic labeling from yeast and cell culture models to primary cells including neurons. Enrichment-free techniques have also been developed that either alkylate the s^4U (SLAM-seq,(Herzog et al., 2017) or recode the hydrogen bonding pattern of s^4U (TimeLapse-seq, (Schofield et al., 2018) in order to induce T-to-C mutations in genome-wide RNA-seq experiments. These techniques offer an additional layer to mRNA 3'end sequencing (Herzog et al., 2017) and total RNA-seq (Schofield et al., 2018) by identifying new RNAs. Importantly nucleoside recoding approaches have been shown to be compatible with traditional enrichment-based techniques (Schofield et al., 2018), thereby combining the ability to enrich rare transcripts with stringent filtering of new reads over nonspecific background.

Here we review recent advances in s^4U metabolic labeling techniques that have been used for global analysis of RNA population dynamics. We have limited our discussion to methods

that have already been applied to genome-wide studies; while many other methods in principle can be extended to genome-wide, it is difficult to predict how much optimization is required in practice to establish compatibility with next-generation sequencing platforms. In addition, we present readers with important considerations and existing challenges when designing genome-wide s^4U metabolic labeling experiments.

STEADY-STATE RNA POPULATION DYNAMICS

When a population of cells are at homeostasis, RNA-seq provides important information about the relative abundance of each RNA, which offers a transcriptome-wide snapshot of the steady-state. However, this freeze-frame view of the transcriptome does not capture the rich dynamics of RNA turnover that are required for cells to remain at homeostasis. In addition, mechanisms for maintaining the steady-state contribute to our understanding of how cells dynamically change their transcriptome in response to changes in their environment. For instance, transcription factors and histone mRNAs tend to be rapidly transcribed and degraded, whereas transcripts involved in cellular metabolism tend to exhibit slower turnover (Yang et al., 2003). Standard RNA-seq experiments are unable to decipher mechanisms of RNA processing and regulation, particularly when cells are at the steady-state. In order to measure transcription and degradation genome-wide, s^4U can be used to label newly transcribed RNAs. Importantly, only transcripts that are actively being transcribed will incorporate s^4U during the feed, which has implications for low abundance transcripts or transcripts that are tissue and/or cell cycle dependent. As there are many different ways to design a metabolic labeling experiment, each with unique acronyms, we instead provide modules for each step of the experiment in Figure 1. We also discuss considerations and challenges when designing and interpreting s^4U metabolic labeling experiments for cells at the steady-state.

Cellular incorporation of s^4U

To study RNA turnover, s^4U can be added to cell culture media at a range of times and concentrations depending on the desired application (Russo, Heck, Wilusz, & Wilusz, 2017). The nucleobase 4-thiouracil can be used as a metabolic labeling reagent in any cell line that expresses UPRT, including *S. cerevisiae* and some archaea (Knüppel, Kuttenberger, & Ferreira-Cerca, 2017), while the nucleoside 4-thiouridine is readily uptaken by mammalian cells and converted into s^4UTP by the endogenous nucleotide salvage pathway. Exogenous nucleoside transporters can be expressed in order to facilitate more efficient uptake of s^4U (C. Miller et al., 2011; Swiatkowska et al., 2012). Finally, while s^4UTP does not readily cross cell membranes due to its charge, s^4UTP has been directly injected into zebrafish embryos for RNA metabolic labeling (Heyn et al., 2014).

While metabolic labeling experiments have been successful across a range of conditions, labeling time and s^4U concentration are critical parameters to consider when designing an experiment in addition to sequencing depth and variability in enrichment (see below). RNA metabolism can be studied via approach-to-equilibrium, where cells are harvested at different times following the addition of s^4U until labeling approaches the steady-state (Figure 1C), or single time point analyses, where the relative populations of s^4U-RNA and

unlabelled RNA allow the calculation of RNA synthesis and decay rates for each transcript. Ideally, the length of s^4U metabolic labeling should be tuned in these cases such that the desired population of transcripts contain 15-90% new RNA (that has been labeled with s^4U) at the end of the labeling period (Russo et al., 2017). Short labeling times decrease the amount of s^4U-RNA available for analysis. This complicates handling and increasing concerns about contamination from non-s^4U-labeled RNAs, although short labeling times also provide the greatest differences for certain RNAs from the steady-state. Long labeling times will eventually lead to labeling of the entire RNA population and reflect the steady-state levels. This will obscure the different kinetics in regulated RNA turnover that these experiments are designed to study, although more s^4U-RNA generally improves the enrichment step. For analysis of individual transcripts, maximum sensitivity is achieved using a labeling time of approximately one half-life (Russo et al., 2017).

Alternatively, a pulse-chase approach can be used to study RNA stability, where cells are labeled with s^4U for several hours (pulse), followed by the addition of a molar excess of uridine (chase) in order to inhibit further incorporation of s^4U into new transcripts (Figure 1B). Cells are harvested at different times following the addition of uridine, and the relative proportion of s^4U-RNA remaining can be fit to a single exponential decay function that reveals the half-life of the RNA. While ideally the length of the pulse should not affect the calculation of RNA half-life because s^4U incorporation is assumed to be a homogenous process, in practice different sub-populations of RNA may have different s^4U labeling and in this case a shorter pulse can be problematic. Therefore, we recommend that the length of s^4U pulse be tuned such that most transcripts are at the steady-state of s^4U incorporation.

The accuracy achieved when determining a half-life for an RNA also depends on the abundance of the RNA and sequencing depth. Different RNA species have different half-lives and no one labeling time is optimal for all RNAs in a genome-wide experiment. Therefore, the time of labeling should be adjusted for the RNA species of interest (Figure 1A). For example, very transient RNAs like introns, enhancer RNAs and antisense transcripts are ideally captured following 5 min of s^4U (Schwalb et al., 2016), whereas most mRNAs can be sufficiently labeled following minutes to hours of s^4U treatment (Russo et al., 2017; Schofield et al., 2018). For very stable transcripts (including most mature miRNAs), a much longer s^4U treatment (several hours to days) may be helpful (Duffy et al., 2015). In an ideal experiment, the absolute RNA half-life should not change with the labeling time, and half-lives of RNAs between different experiments with different labeling times should be comparable. However, in practice different types of experimental bias (see below) can influence RNA half-life measurements, and therefore comparing the relative half-lives of RNAs within a single experimental condition can be more reliable than comparing the absolute half-lives of RNAs between different experiments. In addition, s^4U incorporation has been demonstrated to vary widely by cell type (Russo et al., 2017), so the desired s^4U incorporation for a given cell type should be determined empirically, either by qPCR of a short-lived transcript or by directly quantifying the incorporation of s^4U by dot blot or mass spectrometry (Dölken et al., 2008; Hafner et al., 2010).

s^4U-RNA isolation and handling—RNA handling is critical to analysis of s^4U RNA, and while many of the considerations are the same as for handling unlabeled RNA

(Madabusi, Latham, & Andruss, 2006), there are additional considerations when working with s^4U-RNA. In some cases, the presence of s^4U can lead to selective loss of these subpopulations while handling, resulting in loss of new transcripts. The thiol of s^4U has the potential to form disulfides and/or oxidation products during RNA isolation and handling, and several protocols recommend the addition of reducing agents such as dithiothreitol (DTT) or β-mercaptoethanol (β-me) during RNA isolation (Duffy & Simon, 2016; Schofield et al., 2018; Spitzer et al., 2014). Care should be taken to effectively remove these added reducing reagents before downstream enrichment and/or nucleoside recoding to prevent interfering with the s^4U-specific thiol chemistry.

Potential s^4U toxicity—While s^4U has generally been found to cause minimal toxicity in the cells, some reports have revealed that s^4U can be toxic to certain cell types at high concentrations. For example, s^4U has been reported to cause nucleolar stress in human U2OS cells treated with as little as 50 μM s^4U (Burger et al., 2013). However, this cellular toxicity has not been widely observed in different cell types, even at higher s^4U concentrations (Duffy et al., 2015; Gregersen et al., 2014; Herzog et al., 2017; Russo et al., 2017; Schofield et al., 2018). In addition, cells treated with s^4U for longer labeling times are more likely to exhibit cellular toxicity. Therefore, lower concentrations of s^4U are desirable for longer labeling, whereas higher concentrations of s^4U <u>may not cause adverse effects if the labeling time is very short (i.e. minutes).</u> These concerns can be addressed by conducting s^4U toxicity studies (for examples see (Burger et al., 2013; Schofield et al., 2018) when performing s^4U metabolic labeling in a new cell type or at a higher concentration than previously reported. A summary of tested s^4U concentrations in different cell types has been previously reported (Russo et al., 2017) which we have updated and expanded in Table 1. While the source of cell type-specific differences in cellular toxicity in the presence of s^4U and other metabolic labeling reagents (e.g. BrU, EU) remain unknown, potential sources of variability include reagent cellular permeability and active transport across the cell membrane, biochemical incorporation into the available UTP pool, the rate of total RNA metabolism, potential off-target effects of the reagent and any metabolic derivatives, and possible toxicity of metabolic labeling reagent within RNA, especially ribosomal RNA.

Biochemical enrichment of s^4U-RNA

Choice of activated disulfide reagent—Biochemical enrichment with activated disulfides remains the most common method to identify s^4U-RNAs for genome-wide studies. A key step in s^4U biochemical enrichment is the biotinylation of thiols with activated disulfides. While historically organomercurial matrices were used to purify s^4U-RNA, Cleary *et al.* used HPDP-biotin to enrich metabolically labeled RNA, causing a shift to this reagent for the purification of s^4U-RNAs. Although this activated disulfide has been applied in numerous metabolic labeling experiments, s^4U-RNA enrichment with HPDP-biotin was shown to lead to an enrichment bias (i.e. a skew toward the purification of longer RNAs with more U's). This bias can be corrected for bioinformatically (See (C. Miller et al., 2011; Rabani et al., 2011; Rabani et al., 2014), or through shearing the RNA prior to enrichment (Schwalb et al., 2016). Labeling bias was shown to be one result of inefficient disulfide formation between HPDP-biotin and s^4U, while the more efficient activated

disulfide MTS-biotin alleviates this bias and increases yields in s⁴U-RNA enrichment (Figure 2).

While there are now approaches to mitigate bias in enrichment, given the number of reports using HPDP-biotin without pre-shearing of the RNA, it is worth considering how HPDP-biotin significantly biases RNA capture toward longer RNAs. Unspliced pre-mRNAs can be significantly longer than spliced mRNAs, and an over-estimation of introns in newly transcribed RNA compromises accurate estimation of processing rates. In addition, lower enrichment yields complicate the calculation of RNA half-lives in methods where rates of transcription, processing and degradation are modeled based on the relative proportion of new RNA (enriched fraction) to pre-existing RNA (not captured fraction), although relative rates between different transcripts are still accurate. Therefore, although issues from labeling bias can be mitigated by bioinformatic modeling or biochemical shearing, an efficient biochemical purification of RNA or enrichment-free chemistry is preferable.

Nonspecific RNA background—All biochemical purifications seek to maximize the amount of real signal (in this case s⁴U-RNA) and minimize background contamination (non-s⁴U-RNA). Non-specific contamination has been estimated in some s⁴U-RNA enrichment protocols as high as 30% (Rabani et al., 2011), which can complicate quantification of new RNAs, particularly splicing rates as highly abundant mRNAs are most likely to contribute to background contamination. Many groups have found different ways to overcome challenges associated with nonspecific background in s⁴U-RNA enrichment (summarized in Box 2), including pre-blocking beads with polyvinylpyrrolidone (Pai et al., 2017) or glycogen (Swiatkowska et al., 2012), adding more stringent rinses to the streptavidin beads after incubation with biotinylated RNA (Li et al., 2017), and pre-shearing RNA before biochemical enrichment (Duffy & Simon, 2016). Notably, while RNA pre-shearing is not necessary for all metabolic labeling experiments, this fragmentation step is particularly important following short s⁴U labeling (5 min or less) in order to capture only the portion of the transcript that was newly made during the labeling period. For these very short experiments, failure to fragment RNA before enrichment leads to a 5' bias in RNA coverage (Schwalb et al., 2016).

Others have opted to compare s⁴U-RNA signal to RNA enriched from cells that were not treated with s⁴U, as nonspecific background can be bioinformatically calculated from s⁴U-RNA samples (Barrass et al., 2015). However, this strategy only accounts for nonspecific background on the beads and does not account for unlabeled RNA that is retrieved through base pairing with s⁴U-RNA. Therefore, background contamination may be underestimated by this approach.

A strategy to avoid the multiple steps required for biotinylation, purification and capture has been developed where MTS activated disulfide was directly coupled to magnetic sepharose, allowing for more stringent rinses and higher fold enrichment of s⁴U, which is particularly advantageous for small-scale RNA samples including primary tissues and microdissections (Duffy et al., 2018). When using this MTS-resin for s⁴U-RNA enrichment, we have observed variable amounts of length bias which is not observed with MTS-biotin (Duffy et

al., 2015), although these concerns can be addressed by shearing the RNA prior to enrichment.

In addition, nucleoside recoding can be used to filter non-specific background in biochemically enriched s^4U-RNA during sequencing (Schofield et al., 2018). In a 5 min s^4U metabolic labeling experiment, where the relative proportion of newly transcribed RNA to total RNA is low and enrichment is desirable, nucleoside recoding chemistry was applied to enriched RNA to identify bona fide metabolically labeled RNAs via T-to-C mutations in sequencing. These analyses revealed that, with MTS-biotin enrichment and RNA shearing, nonspecific RNA contamination still comprised 18% of the total signal, but with mutational information these two populations could be analysed separately and new RNAs could be validated in two independent ways (enrichment and T-to-C mutation content). Therefore, we recommend the addition of nucleoside recoding chemistry as a gold-standard for reducing nonspecific RNA background in s^4U-RNA enrichment experiments.

Bioinformatic analysis of enriched s^4U-RNAs—Bioinformatic analysis of s^4U-RNA is largely similar to traditional RNA-seq, the best practices for which have been reviewed elsewhere (Madabusi et al., 2006). Reads are aligned to a reference genome and transcript annotation, and expression levels are quantified. However, several parameters are unique to s^4U enrichment and genome-wide sequencing. As discussed above, the incorporation rate of s^4U into transcripts of interest and little variability in biochemical enrichment is important for robust bioinformatic quantification. In addition, the accuracy of quantification depends on many factors including the depth of sequencing (i.e. the number of reads that map to the transcripts of interest), normalization between samples (particularly those with different s^4U content), and in some cases the ability to identify transcripts from transiently expressed RNA species. These bioinformatic considerations, in conjunction with experimental design and biochemical enrichment, are critical for the interpretation and reproducibility of s^4U metabolic labeling experiments.

Unstable transcript identification—Metabolic labeling experiments with short s^4U labeling (< 1h), enriches for unstable RNAs including enhancer RNAs (eRNAs), antisense transcription at promoters (uaRNAs), and introns from nascent transcripts, which allows the study of transcription output in cells. These unstable RNA species are difficult to detect in the steady-state population because they are rapidly degraded after transcription and/or processing, and their steady-state levels are very low. Therefore, these transcriptional features are typically not included in gene annotations, so alternative methods are required to accurately quantify unstable transcripts in short s^4U labeling experiments. Prior knowledge of the genomic context can aid in the quantification of unstable transcripts; for instance, the presence of CREB-binding protein (CBP) and H3K4me1 was used to identify thousands of activity-dependent enhancers in neurons (Kim et al., 2010). However, for this analysis only regions 1.5 kb from the CBP binding site are considered, so the length of the RNA is not determined using this analysis. In principle, unspliced RNA species including eRNAs, uaRNAs and pre-mRNAs can be identified in regions of continuous transcription. In practice, however, insufficient read depth or repetitive elements within a transcript can affect read mappability and lead to an under-estimation of unstable transcripts when requiring

continuous transcription for quantification. Alternatively, several pipelines have been developed that use hidden Markov modeling (HMM) to identify transcriptional units independent of a known transcript annotation or prior knowledge of the genomic context of the transcript (for examples, see (Chae, Danko, & Kraus, 2015; Heinz et al., 2010; Spitzer et al., 2014; Zacher et al., 2017). Bioinformatic methods that were developed to analyze nuclear run-on sequencing data (GRO-seq and PRO-seq) have also been applied successfully to s^{4}U sequencing data, such as identifying intergenic pri-miRNA transcripts (Duffy et al., 2018), suggesting that the general principles of HMM transcript identification are applicable to multiple metabolic labeling strategies, although depth of sequencing and mappability of repeat elements should be considered for these analyses as well.

Normalization—RNA-seq libraries can be normalized based on reads per kilobase per million reads (RPKM), but s^{4}U-RNA samples cannot be directly compared to RNA-seq or even other s^{4}U-RNA samples when different lengths of s^{4}U labeling time are used (Figure 3A). Therefore, an exogenous spike-in must be used to normalize different s^{4}U-RNA-seq samples in order to bioinformatically compare them. In order to control for variability in handling during s^{4}U-RNA enrichment, an exogenous s^{4}U-labeled RNA spike-in can be added before biotinylation, although in theory these spike-ins can be added during cell lysis to control for variability in total RNA purification as well. For the study of mammalian or *S. cerevisiae* RNA dynamics, *S. pombe* cells can be labeled with s^{4}U and the same amount of s^{4}U-labeled *S. pombe* RNA is added to each experimental sample of 4-thiouracil-treated *S. cerevisiae* cells (Sun et al., 2012). Following enrichment, the samples can be analyzed by a custom microarray for both *S. pombe* and *S. cerevisiae*, where *S. cerevisiae* s^{4}U-RNA levels are normalized by setting the median intensity of *S. pombe* s^{4}U-RNA for all samples equal to 1. A similar strategy was be used for a high-throughput sequencing format ; 4-thiouracil-labeled *S. cerevisiae* RNA was added to HEK293T s^{4}U-RNA samples, and the resulting RNA was sequenced and normalized based on the upper quantile of expression for the *S. cerevisiae* s^{4}U-RNA spike-in (Gregersen et al., 2014). *In vitro* transcribed spike-ins can also be synthesized with s^{4}U by adding s^{4}UTP to the transcription reaction (Munchel et al., 2011; Neymotin et al., 2014), followed by addition to total RNA and identification by high-throughput sequencing (Figure 3A).

While in principle, normalization with exogenous spike-ins, either synthetic or from *S. pombe*, are an effective way to normalize different s^{4}U-RNA levels from different times of metabolic labeling, in practice the normalization has been shown to be variable (Lugowski, Nicholson, & Rissland, 2018). Specifically, small variability in enrichment from cells labeled with s^{4}U-RNA for only a few minutes can significantly influence synthesis and degradation rates in an enrichment-independent manner. An alternative strategy uses introns to normalize between s^{4}U-RNA samples in order to avoid potential variability from exogenous spike-ins (DRUID, Lugowski et al., 2018). Enrichment-free methods based on chemistry that recodes s^{4}U to induce mutations (discussed below) can also alleviate these normalization issues, as information about steady-state transcripts and new RNAs are included in the same sample and traditional normalization strategies for RNA-seq libraries can be used to compare different samples.

Calculating rates of RNA metabolism—The final step of any genome-wide s^4U metabolic labeling experiment is to use the quantification of s^4U-RNAs in order to gain insight into RNA metabolism. Consequently, the models used to calculate these rates of transcription, processing and degradation should be considered carefully. While considerable progress has been made in developing computational algorithms to analyze metabolic labeling data, most models have relatively simple assumptions, which may not accurately reflect the kinetics of RNA metabolism. For example, many RNA decay assays, including s^4U pulse-chase, assume simple first-order decay kinetics. RNA turnover assays that compare a single sample of enriched s^4U-RNA to the steady-state assume that all s^4U-RNA has been captured (Dölken et al., 2008), while enrichment with HPDP-biotin was later shown to be inefficient at capturing s^4U-RNA, resulting in an under-estimation of the proportion of new transcription (Duffy et al., 2015). In addition, while properties of RNA metabolism can be studied using many variations of s^4U metabolic labeling (see Figure 1), very few studies have directly compared the relative power of different methods side-by-side for the ability to accurately reflect absolute rates of RNA metabolism. Therefore, the same techniques reviewed here are the ones necessary to tease apart these differences.

Enrichment-free identification of s^4U-RNA

Many of the challenges identifying s^4U-RNAs through biochemical enrichment can be avoided by chemical techniques that allow nucleotide recoding (Herzog et al., 2017; Riml et al., 2017; Schofield et al., 2018). Chemical treatment of s^4U-RNA can be used to convert s^4U into a nucleotide with an altered hydrogen bonding pattern that is more likely to be read as a C during reverse transcription. Two chemical approaches that rely on different types of chemical reactivity have been developed to globally map sites of s^4U incorporation across the transcriptome (Figure 4A). These approaches provide opportunities to identify s^4U-RNAs that are complementary to enrichment-based approaches (Herzog et al., 2017; Schofield et al., 2018).

Sites of s^4U lead to low levels of T-to-C mutations upon reverse transcription (Hafner et al., 2010; Rabani et al., 2014) but these mutation levels are too low to identify most s^4U-labeled transcripts. To increase the frequency of apparent U-to-C transitions, the s^4U hydrogen bonding pattern can be chemically recoded. The tendency of s^4U to chemically convert to products that produce T-to-C mutations in sequencing experiments has been used as part of photoactivatable ribonucleoside-enhanced crosslinking and immunoprecipitation (PAR-CLIP) to map protein-RNA interactions at nucleotide resolution (Ascanno, Hafner, Cekan, Gerstberger, & Tuschl, 2012; Hafner et al., 2010). Chemistry specifically developed to induce U to C mutations in global sequencing experiments has been developed based on the two chemical strategies: (1) Alkylating the thione of s^4U to make a S4-alkyl-thiouridine (Herzog et al., 2017) (2) oxidize the thione of s^4U to create a leaving group, which allows an amine to substitute into the ring yielding a N4-alkyl cytidine analogue (Schofield et al., 2018).

Chemistry to induce T-to-C mutations during sequencing—In the case of alkylation chemistry, the thione of s^4U can act as a nucleophile. The nucleophilicity of the thione is also the basis of the disulfide chemistry described above. While other bases in RNA

can be alkylated, especially N7 of guanosine (reviewed by (Gillingham, Geigle, & Anatole von Lilienfeld, 2016), early work demonstrated that s4U in E. coli tRNA could be specifically alkylated with chemical labels based on alkyl halides (Hara, Horiuchi, Saneyoshi, & Nishimura, 1970). For the purposes of nucleotide recoding, alkylation of the thione traps thiouridine in a tautomer with one of the hydrogen bonds recoded (from acceptor-donor-acceptor to acceptor-acceptor-acceptor, Figure 4B). This alkylation results in a base that is more likely to be read as C than U during reverse transcription. The use of iodoacetamide was developed for identifying sites of s4U in RNA in 3'-ends of RNA across the transcriptome (SLAM-seq, (Herzog et al., 2017), allowing analysis of s4U-RNA including the steady state RNA dynamics of poly-adenylated RNAs.

Alternatively, the hydrogen bonding of s4U can be fully recoded using oxidative nucleophilic aromatic substitution. In this case the thione of s4U is oxidized to create a leaving group which can be displaced with alkylamines to make cytidine analogues. Oxidative nucleophilic aromatic substitution chemistry was first used with s4U to specifically modify *E. coli* tRNA s4U bases (Ziff & Fresco, 1969), (Hayatsu & Yano, 1969). Extending this reactivity for use transcriptome-wide involved migrating from strong oxidants such as $KMnO_4$ to more specific oxidants such as $NaIO_4$ (Schofield et al., 2018). Similarly, while the use of ammonia provides the bone fide cytidine product (Hayatsu & Yano, 1969; Riml et al., 2017), amines with lower pKa values such as trifluoroethylamine can be used that remain deprotonated at neutral pH values. We refer to this reactivity as TimeLapse chemistry. The effect of TimeLapse chemistry is to convert s4U to cytosine analogues, resulting in complete recoding of s4U from the pattern of U to the pattern of C (from acceptor-donor-acceptor to donor-acceptor-acceptor). TimeLapse-seq was validated to monitor the location of s4U in transcriptome-wide RNA-seq experiments where intronic reads, non-poly-adenylated RNAs, and different transcript isoforms could be observed (Schofield et al., 2018).

Both alkylation and TimeLapse chemistry efficiently convert s4U to their respective analogue (s4U* or C*). While the mutation rate in the context of a complex RNA mixture has not been determined for either approach, both reactions convert the majority of s4U in model substrates. Reverse transcriptase enzymes have a non-zero termination rate for even natural nucleotides, so it is reasonable to wonder if the adducts induced by these transformations (S4-alkyl thiouridine for SLAM-seq, and N4-alkyl cytidine for TimeLapse-seq) induce an increase in termination in reverse transcriptase reactions. When analyzed using test substrates, neither SLAM-seq nor TimeLapse-seq led to a substantial increase in termination of reverse transcription at modified bases. The importance of full versus partial recoding of the s4U hydrogen bonding pattern will require a side-by-side analysis of both methods, which has not yet been published.

Bioinformatic analysis of T-to-C mutations—After conversion of s4U to s4U* or C*, the reverse transcriptase records the site of s4U as a G in the cDNA, and these locations are identifiable as T-to-C mutations in sequencing data. Ideally all sequencing reads could be classified as either resulting from metabolically labeled s4U-RNA or as unlabeled RNA. The combination of s4U treatment conditions and chemistries that have been developed generally lead to 1-10% T-to-C mutation rates. These rates are low enough to avoid substantial

problems during read alignment using standard pipelines. Under conditions where 2% of uridines are substituted with s^4U and result is chemically induced T-to-C mutations, many reads from metabolically labeled transcripts will have zero mutations (as predicted from a binomial distribution). For example, in a sequencing experiment with a single-end 50 nt reads, with a 2% mutation rate less than a quarter of the reads (22%) are expected to contain s^4U-induced mutations. The number of reads with mutations can be increased by increasing s^4U incorporation rates (e.g., higher [s^4U] treatments) or by using a longer sequencing format. In the example here, switching from a single-end 50 nt format to a paired-end 150 nt format substantially increases the fraction of s^4U-RNA reads expected to contain mutations (from 22% to 78%). The 1-10% T-to-C mutation rates observed in these experiments is well above background rates which vary experiment to experiment but tend to be less than 0.2% using standard RNA-seq workflows. It is worth noting that even these low background rates of T-to-C mutations can become problematic when there are very high numbers of unlabeled transcripts. For example, if only 1% of a transcript is labeled with s^4U, the background mutations from unlabeled transcripts will frequently outnumber the s^4U induced mutations.

There are two approaches that have been used to analyze steady state RNA dynamics from nucleotide recoding experiments with s^4U: (1) using averaged mutation rates (Herzog et al., 2017); or (2) single-molecule analysis of sequencing reads using statistical modeling (Schofield et al., 2018). The first approach (using averaged mutation rates) was applied to a chase-style experiment where cells were treated for a long time with s^4U (100 μM for 12h) prior to a chase with uridine. The change in background-subtracted average mutation rates over time was used for curve fitting to determine the RNA half-lives.

Alternatively, statistical modeling can be used to take advantage of single-molecule information that is inherent to techniques such as TimeLapse-seq (Schofield et al., 2018). This information is lost when T-to-C mutation rates are averaged. Each sequencing read reports on a single RNA transcript that was either s^4U-labeled or unlabeled. The distribution of the number of T-to-C mutations in each read can be used to infer the likelihood that the read came from an RNA was labeled (Schofield et al., 2018). The distribution of mutations can be modeled as a mixture of two populations: labeled and unlabeled RNA molecules. These single-molecule distributions can be modeled using either a Poisson (using the rate of mutations per read) or a binomial model (which accounts for the number of uridines in each read). The background distributions can be determined from control experiments, and the mutation rates of s^4U-labeled RNAs can be inferred from the data. Using likelihood maximization or bayesian hierarchical modeling, the fraction of each transcript (or other feature such as exon) that was labeled with s^4U can be inferred with high reproducibility. The advantage of using single molecule information from the sequencing reads is particularly apparent in cases where only a small fraction of RNA is labeled. In this case, the average T-to-C mutation rate is very close to background levels, yet the increase in mutations from the labeled RNAs is apparent from the ratios of different numbers of mutations, including high numbers of mutations (which are very rare in unlabeled reads; in the example in Box 3 less than 0.002% of reads derived from pre-existing transcripts have three or greater mutations). By treating the data as single-molecule data, the frequency of mutations can be used to reproducibly infer even small fractions of labeled RNA.

Nucleotide recoding as a method to identify s⁴U-RNA offers several advantages over enrichment-based techniques. Nucleotide recoding requires fewer steps than biochemical approaches and many samples can be processed in parallel. Because there is no need for biochemical purification, these approaches can be performed on very little input RNA—orders of magnitude less RNA than is generally required for biochemical enrichment. One particularly useful advantage is that all the reads are sequenced in the same experiment; the data are internally normalized, avoiding the challenges described above. For nucleotide recoding approaches to be effective, the total amount of s⁴U-labeled material that is sequenced needs to be a significant fraction of a sequencing lane. Very short s⁴U treatments (such as the 5 min transient transcriptome sequencing) produce very few reads that have T-to-C mutations, and therefore biochemical enrichment is still advantageous. Even in cases that require biochemical enrichment, however, including nucleotide recoding after enrichment is useful to distinguish real signal from contaminating non-s⁴U-labeled background.

EXTENSIONS OF TRANSCRIPTIONAL ANALYSIS

Induced changes in RNA metabolism

While s⁴U metabolic labeling does not require the induction of genes or the use of reporters, many of the methods described above can be used to measure changes upon cellular perturbation as well as steady-state RNA population dynamics. For instance, s⁴U metabolic labeling has been used with s⁴U treatment at multiple time points following interferon (INF) stimulation in mouse embryonic fibroblasts (Dölken et al., 2008), lipopolysaccharide (LPS) stimulation in dendritic cells (Rabani et al., 2011), and interleukin-7 stimulation in naïve T-cells (Li et al., 2017) in order to assess the relative contribution of transcription and processing to the changes in RNA steady-state levels that occur upon stimulation. Analogous methods have been applied in *S. cerevisiae* to measure transcriptional changes upon osmotic stress (C. Miller et al., 2011) and Ccr4-Not knockout (Sun et al., 2012). In addition, enrichment-free nucleoside conversion has been used to observe transcriptional changes after 1 hour of heat shock in MEF cells, which revealed induction of heat shock transcripts that were not detectable by RNA-seq alone at this short time scale (Schofield et al., 2018).

An important component of these protocols is using bioinformatic analyses to assess the relative contribution of transcription, processing, and decay to changes in total RNA levels. To model synthesis, processing, and degradation rates, Rabani et al. developed a computational approach that infers degradation rates based on steady-state RNA levels from total RNA and s⁴U-RNA populations (Rabani et al., 2014). The simplest model ("constant degradation") assumes that no degradation of s⁴U-RNA occurs during the metabolic labeling period, whereas the "varying degradation" model assumes that degradation occurs during labeling. Transcripts that significantly reject the constant degradation model are highly transient, so the degradation rate significantly contributes to changes in steady-state levels. Processing rates can be estimated by comparing the ratio of intronic reads to spliced reads that contain exon-exon junctions. These methods were later refined and formalized into publicly available computational pipelines available in different programming languages (DRiLL (Rabani et al., 2014) is available in MATLAB, and INSPeCT (de Pretis et al., 2015)

in R). Therefore, small changes in experimental design and bioinformatic analysis can easily extend our understanding of steady-state RNA dynamics to mechanisms of inducible changes in RNA metabolism that allow cells to respond to the surrounding environment.

RNAPII elongation

Recent genome-wide experiments have revealed that RNAPII pausing, as well as the rate of elongation following release from pausing, are tightly coupled to co-transcriptional processes such as splicing, termination, and RNA stability (reviewed by (Jonkers & Lis, 2015). Measuring RNAPII elongation rates genome-wide requires quantifying the distance that the polymerase travels as a function of elapsed time. This can be achieved by treatment with 5,6-dichloro-1-β-D-ribofuranosylbenzimidazole (DRB), a small molecule that inhibits pTEFb phosphorylation and therefore prevents RNAPII from releasing from the pause site into productive elongation. Even if s^4U is added during the DRB treatment, a paused polymerase will not incorporate s^4U. Upon washout of DRB, new transcripts are labeled with s^4U, and cells are harvested at multiple times following washout. Because RNAPII becomes effectively synchronized at the pause site during DRB treatment, the distance RNAPII travels directly measures the elongation rate, and rates can be measured genome-wide (Fuchs et al., 2014). RNAPII elongation rates calculated by this method are unable to detect variations in elongation within genes, and only relatively long genes can be used. During the same metabolic labeling period, RNA produced from small genes would be synthesized and exported to the cytoplasm faster than larger genes, and therefore the rates of RNAPII elongation at these short genes requires temporal resolution that is not currently feasible. Regardless, genome-wide DRB-seq methods offer improvements over previous methods that use RT-PCR (Singh & Padgett, 2009) or fluorescent labeling (Darzacq et al., 2007) to measure elongation rates of only a handful of genes at a time. In addition, DRB inhibition combined with s^4U metabolic labeling was recently used to demonstrate that genome-wide variation in RNAPII elongation rate is consistent between cell culture models and mouse primary neurons (Duffy et al., 2018).

Tissue-specific transcription

In addition to capturing new RNAs with temporal resolution, s^4U metabolic labeling can also be leveraged for spatial resolution of new transcripts in a whole organism (TU-tagging, (M. R. Miller, Robinson, Cleary, & Doe, 2009). The UPRT enzyme, which converts 4-thiouracil into 4-thio-UTP, can be expressed in the cell type of interest via targeted transgene expression, followed by injection of the nucleobase 4-thiouracil (4TU). Only cells that express the UPRT transgene are able to incorporate 4TU into newly transcribed RNA, thus allowing cell type-specific RNA enrichment from whole tissues. While in principle TU tagging can also give temporal resolution of transcripts via the methods described above, in practice the kinetics of 4TU incorporation into new transcripts in a whole organism are not well characterized, which may complicate analyses of RNA stability or transcription rate. Regardless, this approach is particularly advantageous over methods that isolate cell type specific translating ribosomes (TRAP,(Heiman et al., 2008) because TU tagging captures non-coding RNAs in addition to protein coding transcripts, or methods that isolate cell-specific nuclei (INTACT,(Deal & Henikoff, 2010) because only nuclear RNAs are detected.

Conclusion

Methods that enable the study of RNA population dynamics give a rich picture of how steady-state RNA levels are regulated and how cells dynamically respond to environmental stimuli. 4-thiouridine has proven to be a versatile metabolic label for understanding RNA transcription, processing and degradation in a variety of organisms. For example, short pulses of s^4U have been used to measure differences in transcriptional efficiency of TATA-less versus TATA-containing promoters in yeast (Donczew & Hahn, 2018) as well as the influence of the RNA helicase DDX54 on pre-mRNA splicing efficiency in response to DNA damage (Milek et al., 2018). RNA half-life measurements have demonstrated the contribution of RNA helicase MOV10 RNA stability (Gregersen et al., 2014) as well as the importance of m^6A to regulate RNA stability during interleukin-7-dependent T-cell maturation (Li et al., 2017). Approach-to-equilibrium experiments have helped to identify cellular factors that facilitate rapid mRNA degradation in response to changes in environmental nitrogen in *S. cerevisiae* (D. Miller, Brandt, & Gresham, 2018) and revealed a subset of mature miRNAs with rapid turnover in proliferating HEK293T cells (Duffy et al., 2015). In addition, transcript isoforms like ASXL1 in human cells have been shown to have different stabilities, which suggests that differential isoform stability may be a more widespread consequence of alternative splicing (Schofield et al., 2018).

These methods can also be modified and combined to add additional power to s^4U-RNA identification, as demonstrated in Figure 1. For example, tissue-specific expression of the UPRT enzyme enables the spatial and temporal analysis of RNA dynamics in living organisms (TU-tagging). In general, these strategies are also compatible with other RNA-seq workflows. For example, s^4U-RNAs enriched after a short pulse of s^4U can be treated with nucleoside recoding chemistry in order to bioinformatically filter out nonspecific RNA background using the presence of T-to-C mutations in enriched reads (TT-TimeLapse-seq, Schofield et al. 2018). Enrichment is required in these cases in order to detect the small proportion of s^4U-RNAs that would not be abundant enough to easily detect with nucleoside recoding strategies alone, and the addition of T-to-C mutations in the RNA-seq data allows the precise calculation of RNA contamination levels and removal of non-s^4U reads from downstream analysis. Given that all of the information from biochemical enrichment experiments is retained when T-to-C mutations are added, there is good reason to apply recoding chemistry when performing biochemical enrichment experiments.

We anticipate that recent improvements to s^4U metabolic labeling techniques, including more efficient chemistry, single-step capture of s^4U, improved normalization strategies and enrichment-free nucleoside conversion chemistry, will provide a robust toolkit of experimental strategies to understand RNA population dynamics in many biological contexts. Recent advances in single-cell RNA sequencing also present the opportunity to apply s^4U metabolic labeling to understand cellular heterogeneity of RNA population dynamics. In addition, improvements to sample normalization, as well as the addition of nucleoside conversion chemistry to filter nonspecific RNA contamination, should enable more robust measurements of RNA transcription and processing events genome-wide. With proper considerations for experimental design, RNA handling and bioinformatic analysis,

s^{4}U metabolic labeling holds the power to help reveal the numerous strategies that organisms have evolved in order to regulate RNA population dynamics.

Acknowledgments

References

Ascanno M, Hafner M, Cekan P, Gerstberger S, & Tuschl T (2012). Identification of RNA-protein interaction networks using PAR-CLIP. Wiley Interdisciplinary Reviews: RNA, 3(2), 159–177. doi: 10.1002/wrna.1103 [PubMed: 22213601]

Barrass JD, Reid JEA, Huang Y, Hector RD, Sanguinetti G, Beggs JD, & Granneman S (2015). Transcriptome-wide RNA processing kinetics revealed using extremely short 4tU labeling. Genome Biology, 16, 282. doi: 10.1186/s13059-015-0848-1 [PubMed: 26679539]

Burger K, Mühl B, Kellner M, Rohrmoser M, Gruber-Eber A, Windhager L, … Eick D (2013). 4-thiouridine inhibits rRNA synthesis and causes a nucleolar stress response. RNA biology, 10(10), 1623–1630. doi: 10.4161/rna.26214 [PubMed: 24025460]

Chae M, Danko CG, & Kraus WL (2015). groHMM: a computational tool for identifying unannotated and cell type-specific transcription units from global run-on sequencing data. BMC Bioinformatics, 16, 222. doi: 10.1186/s12859-015-0656-3 [PubMed: 26173492]

Churchman LS, & Weissman JS (2011). Nascent trascript sequencing visualizes trascription at nucleotide resolution. Nature, 469(7330), 368–373. [PubMed: 21248844]

Cleary M, Meiering C, Jan E, Guymon R, & Boothroyd J (2005). Biosynthetic labeling of RNA with uracil phosphoribosyltransferase allows cell-specific microarray analysis of mRNA synthesis and decay. Nature Biotechnology, 23(2), 232–237. doi: 10.1038/nbt1061

Core LJ, Waterfall JJ, & Lis JT (2008). Nascent RNA sequencing reveals widespread pausing and divergent initiation at human promoters. Science, 322(5909), 1845–1848. [PubMed: 19056941]

Darzacq X, Shav-Tal Y, de Turris V, Brody Y, Shenoy SM, Phair RD, & Singer RH (2007). In vivo dynamics of RNA polymerase II transcription. Nature Structural & Molecular Biology, 14, 796–806.

de Pretis S, Kress T, Morelli MJ, Melloni GEM, Riva L, Amati B, & Pelizzola M (2015). INSPEcT: a computational tool to infer mRNA synthesis, processing, and degradation dynamics from RNA- and 4sU-seq time course experiments. Bioinformatics, 31(17), 2829–2835. [PubMed: 25957348]

de Pretis S, Kress T, Morelli MJ, Sabo A, Locarno C, Verrecchia A, … Pelizzola M (2017). Integrative analysis of RNA polymerase II and transcripitonal dynamics upon MYC activation. Genome Research, 27, 1658–1664. [PubMed: 28904013]

Deal RB, & Henikoff S (2010). A simple method for gene expression and chromatin profiling of individual cell types within a tissue. Developmental Cell, 18(6), 1030–1040. doi: 10.1016/j.devcel.2010.05.013 [PubMed: 20627084]

Dölken L, Ruzsics Z, Rädle B, Friedel C, Zimmer R, Mages J, … Koszinowski U (2008). High-resolution gene expression profiling for simultaneous kinetic parameter analysis of RNA synthesis and decay. RNA (New York, N.Y.), 14(9), 1959–1972. doi: 10.1261/rna.1136108

Donczew R, & Hahn S (2018). Mechanistic differences in transcription initiation at TATA-less and TATA-containing promoters. Molecular and Cellular Biology, 38(1), e00448–00417. [PubMed: 29038161]

Duffy EE, Canzio D, Maniatis T, & Simon MD (2018). Solid phase chemistry to covalently and reversibly capture thiolated RNA. Nucleic Acids Res, gky556. doi: 10.1093/nar/gky556

Duffy EE, Rutenberg-Schoenberg M, Stark CD, Kitchen RR, Gerstein MB, & Simon MD (2015). Tracking Distinct RNA Populations Using Efficient and Reversible Covalent Chemistry. Molecular Cell, 59(5), 858–866. doi: 10.1016/j.molcel.2015.07.023 [PubMed: 26340425]

Duffy EE, & Simon MD (2016). Enriching s4U-RNA Using Methane Thiosulfonate (MTS) Chemistry. Current Protocols in Chemical Biology, 8(4), 234–250. doi: 10.1002/cpch.12 [PubMed: 27925666]

Friedel CC, Dolken L, Ruzsics Z, Koszinowski U, & Zimmer R (2009). Conserved principles of mammalian transcription regulation revealed by RNA half-life. Nucleic Acids Research, 37(17), e115. [PubMed: 19561200]

Fuchs G, Voichek Y, Benjamin S, Gilad S, Amit I, & Oren M (2014). 4sUDRB-seq: measuring genomewide transcriptional elongation rates and initiation frequencies within cells. Genome Biology, 15(5), R69. [PubMed: 24887486]

Gillingham D, Geigle S, & Anatole von Lilienfeld O (2016). Properties and reactivity of nucleic acids relevant to epigenomics, transcriptomics, and therapeutics. Chem Soc Rev, 45(9), 2637–2655. [PubMed: 26992131]

Gregersen LH, Schueler M, Munschauer M, Mastrobuoni G, Chen W, Kempa S, … Landthaler M (2014). Mov10 is a 5' to 3' RNA helicase contributing to UPF1 mRNA target degradation by translocation along 3' UTRs. Mol Cell, 54(4), 573–585. doi: 10.1016/j.molcel.2014.03.017 [PubMed: 24726324]

Hafner M, Landthaler M, Burger L, Khorshid M, Hausser J, Berninger P, … Tuschl T (2010). Transcriptome-wide identification of RNA-binding protein and microRNA target sites by PAR-CLIP. Cell, 141(1), 129–141. doi: 10.1016/j.cell.2010.03.009 [PubMed: 20371350]

Hara H, Horiuchi T, Saneyoshi M, & Nishimura S (1970). 4-Thiouridine-specific spin-labeling of E. coli transfer RNA. Biochem Biophys Res Commun, 38(2), 305–311. [PubMed: 4313932]

Hayatsu H, & Yano M (1969). Permanganate oxidation of 4-thiouracil derivatives. Isolation and properties of 1-substituted 2-pyrimidone 4-sulfonates. Tetrahedron Letters, 10, 755–758.

Heiman M, Schaefer A, Gong S, Peterson JD, Day M, Ramsey KE, … Heintz N (2008). A translational profiling approach for the molecular characterization of CNS cell types. Cell, 135(4), 738–748. doi: 10.1016/j.cell.2008.10.028 [PubMed: 19013281]

Heinz S, Benner C, Spann N, Bertolino E, Lin YC, Laslo P, … Glass CK (2010). Simple combinations of lineage-determining transcription factors prime cis-regulatory elements required for macrophage and B cell identities. Mol Cell, 38(4), 576–589. doi: 10.1016/j.molcel.2010.05.004 [PubMed: 20513432]

Herzog VA, Reichholf B, Neumann T, Rescheneder P, Bhat P, Burkard TR, … Ameres SL(2017). Thiol-linked alkylation of RNA to assess expression dynamics. Nature Methods, 14(12), 1198–1204. doi: 10.1038/nmeth.4435 [PubMed: 28945705]

Heyn P, Kircher M, Dahl A, Kelso J, Tomancak P, Kalinka AT, & Neugebauer KM (2014). The earliest transcribed zygotic genes are short, newly evolved, and different across species. Cell Reports, 6(2), 285–292. doi: 10.1016/j.celrep.2013.12.030 [PubMed: 24440719]

Hokin LE, & Hokin MR (1954). The incorporation of 32P into the nucleotides of ribonucleic acid in pancreas slices during enzyme synthesis and secretion. Biochemica et Biophysica Acta, 13, 401–412.

Jao C, & Salic A (2008). Exploring RNA transcription and turnover in vivo by using click chemistry. Proceedings of the National Academy of Sciences of the United States of America, 105(41), 15779–15784. doi: 10.1073/pnas.0808480105 [PubMed: 18840688]

Jonkers I, & Lis JT (2015). Getting up to speed with transcription elongation by RNA polymerase II. Nature Reviews Molecular Cell Biology, 16, 167–177. [PubMed: 25693130]

Kenzelmann M, Maertens S, Haergenhahn M, Kueffer S, Hotz-Wagenblatt A, Li L, … Schütz G (2007). Microarray analysis of newly synthesized RNA in cells and animals. Proc Natl Acad Sci U S A, 104(15), 164–169.

Kim T-K, Hemberg M, Gray JM, Costa AM, Bear DM, Wu J, … Greenberg ME (2010). Widespread transcription at neuronal activity-regulated enhancers. Nature, 465(7295), 182–187. [PubMed: 20393465]

Knüppel R, Kuttenberger C, & Ferreira-Cerca S (2017). Toward time-resolved analysis of RNA metabolism in archaea using 4-thiouracil. Frontiers in Microbiology, 8, 286. doi: 10.3389/fmicb.2017.00286 [PubMed: 28286499]
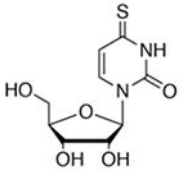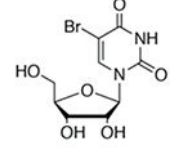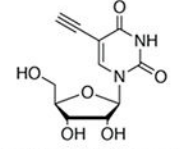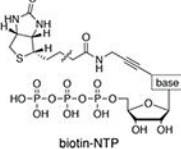
Kwak H, Fuda NJ, Core LJ, & Lis JT (2013). Precise maps of RNA polymerase reveal how promoters direct initiation and pausing. Science, 339(6122), 950–953. doi: 10.1126/science.1229386 [PubMed: 23430654]

Li HB, Tong J, Zhu S, Batista PJ, Duffy EE, Zhao J, … Flavell RA. (2017). m6A mRNA methylation controls T cell homeostasis by targeting the IL-7/STAT5/SOCS pathways. Nature, 548(7667), 338–342. doi: 10.1038/nature23450 [PubMed: 28792938]

Logan JE, Heagy FC, & Rossiter RJ (1955). Phosphorous metabolism of the liver: effect of hypophysectomy, adrenalectomy, and administration of ACTH on the incorporation of radioactive phosphate into RNA nucleotides. Canadian Journal of Biochemistry and Physiology, 33(1), 54–61. [PubMed: 13230950]

Lugowski A, Nicholson B, & Rissland OS (2018). DRUID: a pipeline for transcriptome-wide measurements of mRNA stability. RNA, 24(5), 623–632. doi: 10.1261/rna.062877.117 [PubMed: 29438994]

Madabusi LV, Latham GJ, & Andruss BF (2006). RNA extraction for arrays. Methods Enzymol, 411, 1–14. doi: 10.1016/S0076-6879(06)11001-0 [PubMed: 16939782]

Melvin WT, Milne HB, Slater AA, Allen HJ, & Keir HM (1978). Incorporation of 6-thioguanosine and 4-thiouridine into RNA. Application to isolation of newly synthesised RNA by affinity chromatography. European Journal of Biochemistry, 92(2), 373–379. [PubMed: 570106]

Meryet-Figuiere M, Alaei-Mahabadi B, Ali MM, Mitra S, Subhash S, Pandey GK, … C. K (2014). Temporal separation of replication and transcription during S-phase progression. Cell Cycle, 13(20), 3241–3248. doi: 10.4161/15384101.2014.953876 [PubMed: 25485504]

Milek M, Imami K, Mukherjee N, De Bortoli F, Zinnall U, Hazapis O, … Landthaler M (2018). DDX54 regulates transcriptome dynamics during DNA damage response. Genome Research, 27, 1344–1359.

Miller C, Schwalb B, Maier K, Schulz D, Dümcke S, Zacher B, … Cramer P (2011). Dynamic transcriptome analysis measures rates of mRNA synthesis and decay in yeast. Molecular systems biology, 4(7), 458. doi: 10.1038/msb.2010.112

Miller D, Brandt N, & Gresham D (2018). Systematic identification of factors mediating accelerated mRNA degradation in response to changes in enviornmental nitrogen. PLoS Genetics, 14(5), p1–27.

Miller MR, Robinson KJ, Cleary MD, & Doe CQ (2009). TU-tagging: cell type-specific RNA isolation from intact complex tissues. Nature Methods, 6, 439–441. [PubMed: 19430475]

Munchel SE, Shultzaberger RK, Takizawa N, & Weis K (2011). Dynamic profiling of mRNA turnover reveals gene-specific and system-wide regulation of mRNA decay. Molecular Biology of the Cell, 22(15), 2787–2795. doi: 10.1091/mbc.E11-01-0028 [PubMed: 21680716]

Muramatsu M, & Busch H (1964). Studies on nucleolar RNA of the Walker 25 carcinoma and the liver of the rat. Cancer Research, 24, 1028–1034. [PubMed: 14195340]

Neymotin B, Athanasiadou R, & Gresham D (2014). Determination of in vivo RNA kinetics using RATE-seq. RNA, 20, 1645–1652. doi: 10.1261/rna.045104.114 [PubMed: 25161313]

Pai AA, Henriques T, McCue K, Burkholder A, Adelman K, & Burge CB (2017). The kinetics of pre-mRNA splicing in the Drosophila genome and the influence of gene architecture. Elife, 6, e23537.

Rabani M, Levin JZ, Fan L, Adiconis X, Raychowdhury R, Garber M, … Regev A (2011). Metabolic labeling of RNA uncovers principles of RNA production and degradation dynamics in mammalian cells. Nature Biotechnology, 29(5), 436–442. doi: 10.1038/nbt.1861

Rabani M, Raychowdhury R, Jovanovic M, Rooney M, Stumpo DJ, Pauli A, … Regev A (2014). High-resolution sequencing and modeling identifies distinct dynamic RNA regulatory strategies. Cell, 159(7), 1698–1710. doi: 10.1016/j.cell.2014.11.015 [PubMed: 25497548]

Riml C, Amort T, Rieder D, Gasser C, Lusser A, & Micura R (2017). Osmium-Mediated Transformation of 4-Thiouridine to Cytidine as Key To Study RNA Dynamics by Sequencing. Angew Chem Int Ed Engl, 56(43), 13479–13483. doi: 10.1002/anie.201707465 [PubMed: 28817234]

Russo J, Heck AM, Wilusz J, & Wilusz CJ (2017). Metabolic labeling and recovery of nascent RNA to accurately quantify mRNA stability. Methods, 120, 39–48. doi: 10.1016/j.ymeth.2017.02.003 [PubMed: 28219744]

Schofield JA, Duffy EE, Kiefer L, Sullivan MC, & Simon MD (2018). TimeLapse-seq: adding a temporal dimension to RNA sequencing through nucleoside recoding. Nature Methods. doi: doi: 10.1038/nmeth.4582

Schwalb B, Michel M, Zacher B, Frühauf K, Demel C, Tresch A, … Cramer P (2016). TT-seq maps the human transient transcriptome. Science, 352(6290), 1225–1228. doi: 10.1126/science.aad9841 [PubMed: 27257258]

Schwanhäusser B, Busse D, Li N, Dittmar G, Schuchhardt J, Wolf J, … Selbach M (2011). Global quantification of mammalian gene expression control. Nature, 473, 337–342. [PubMed: 21593866]

Singh J, & Padgett RA (2009). Rates of in situ trascription and splicing in large human genes. Nature Structural & Molecular Biology, 16, 1128–1133.

Spitzer J, Hafner M, Landthaler M, Ascano M, Farazi T, Wardle G, … Tuschl T (2014). PAR-CLIP (Photoactivatable Ribonucleoside-Enhanced Crosslinking and Immunoprecipitation): a Step-By-Step Protocol to the Transcriptome-Wide Identification of Binding Sites of RNA-Binding Proteins In Lorsch J (Ed.), Laboratory Methods in Enzymology: Protein Part B (Vol. 539, pp. 113–161). Methods in Enzymology: Elsevier.

Sun M, Schwalb B, Schulz D, Pirkl N, Etzold S, Larivire L, … Cramer P (2012). Comparative dynamic transcriptome analysis (cDTA) reveals mutual feedback between mRNA synthesis and degradation. Genome Research, 22, 1350–1359. [PubMed: 22466169]

Swiatkowska A, Wlotzka W, Tuck A, Barrass JD, Beggs JD, & Tollervey D (2012). Kinetic analysis of pre-ribosome structure in vivo. RNA, 18, 2187–2200. [PubMed: 23093724]

Tani H, & Akimitsu N (2012). Genome-wide technology for determining RNA stability in mammalian cells. RNA biology, 9(10), 1233–1238. [PubMed: 23034600]

Tani H, Mizutani R, Salam KA, Tano K, Ijiri K, Wakamatsu A, … Akimitsu N (2012). Genome-wide determination of RNA stability reveals hundreds of short-lived noncoding transcripts in mammals. Genome Research, 22(5), 947–956. doi: 10.1101/gr.130559.111 [PubMed: 22369889]

Ussuf KK, Anikumar G, & Nair PM (1995). Newly synthesized mRNA as a probe for identification of wound responsive genes from potatoes. Indian J Biochem Biophys, 32(2), 78–83. [PubMed: 7642204]

Windhanger L, Bonfert T, Burger K, Ruzsics Z, Krebs S, Kauffman S, … Dolken L (2012). Ultrashort and progressive 4sU-tagging reveals key characteristics of RNA processing at nucleotide resolution. Genome Research, 22(10), 2031–2042. [PubMed: 22539649]

Woodford TA, Schlegel R, & Pardee AB (1988). Selective isolation of newly synthesized mammalian mRNA after in vivo labeling with 4-thiouridine or 6-thioguanosine. Anal Biochem, 171(1), 166–172. [PubMed: 3407913]

Yang E, van Nimwegen E, Zavolan M, Rajewsky N, Schroeder M, Magnasco M, & Darnell JEJ (2003). Decay rates of human mRNAs: correlation with functional characteristics and sequence attributes. Genome Research, 13(8), 1863–1872. doi: 10.1101/gr.1272403 [PubMed: 12902380]

Zacher B, Michel M, Schwalb B, Cramer P, Tresch A, & Gagneur J (2017). Accurate Promoter and Enhancer Identification in 127 ENCODE and Roadmap Epigenomics Cell Types and Tissues by GenoSTAN. PLoS One, 12(1), e0169249. doi: 10.1371/journal.pone.0169249 [PubMed: 28056037]

Ziff EB, & Fresco JR (1969). A method for locating 4-thiuridylate in the primary structure of transfer ribonucleic acids. Biochemistry, 8(8), 3242–3248. [PubMed: 4897331]

**Box 1:** Metabolic labeling reagents for the capture of newly transcribed RNA.

 4-thiouridine (s^4U)	S^4U (or 4-thiouracil in cells that express UPRT) is rapidly uptaken by cells, and s^4U-RNA can be enriched with activated disulfide chemistry (e.g. HPDP-biotin [Cleary 2005], MTS-biotin [Duffy 2015], or MTS-resin [Duffy 2018]) or identified by enrichment-free conversion chemistry (Herzog 2017, Schofield 2018). Advantages: activated disulfide chemistry is both efficient and reversible, and enrichment-free chemistry offers single-nucleotide resolution.
 5-bromouridine (BrU)	BrUTP is added to isolated nuclei for rapid uptake and short RNA labeling (Core 2008), while BrU is uptaken by cells at a slower rate and is applicable for pulse-chase experiments (Tani 2012). BrU-RNA is enriched using anti-BrdU antibodies. Advantages: BrU metabolic labeling methods are widely used and well validated. BrU is also compatible with immunostaining (Wansink 1993).
 5-ethynyluridine (EU)	EU is rapidly uptaken into cells, and EU-RNA can be enriched with click chemistry (azide-conjugated biotin) or used for live-cell nascent RNA labeling (Jao 2008). Advantages: 5-EU enrichment chemistry is covalent (although irreversible) and compatible with live-cell imaging.
 biotin-NTP	Biotin-NTPs are added in four separate reactions to isolated nuclei for rapid uptake and short RNA labeling, although all four biotin-NTPs can be added to the same reaction (Kwak 2013). Biotinylated RNA is enriched with streptavidin-coated magnetic beads. Advantages: Single base-pair resolution is achieved for the precise localization of RNA polymerase.

Box 2: Potential sources of nonspecific RNA background and methods to filter this contamination experimentally and bioinformatically.

| Source of background	Experimental strategy
Nonspecific RNA binding to surfaces	• Use low retention tubes • Transfer streptavidin beads or MTS resin to new tube before elution step • Perform nucleoside conversion chemistry after enrichment to identify s^4U-containing reads during bioinformatic analysis
Nonspecific RNA binding to beads	• Fragment total RNA before enrichment • Pre-block beads with polyvinylpyrrolidone or glycogen • Add high salt rinses to RNA on beads • Compare s^4U-RNA to a non-s^4U RNA sample • Perform nucleoside conversion chemistry after enrichment to identify s^4U-containing reads during bioinformatic analysis
Nonspecific RNA base-pairing with s^4U-RNA on beads	• Add low salt and/or denaturing washes to RNA on beads • Perform nucleoside conversion chemistry after enrichment to identify s^4U-containing reads during bioinformatic analysis
Contamination from endogenously thiolated RNAs (e.g. 2-thiouridine-containing tRNA)	• Compare s^4U-RNA to a non-s^4U RNA sample
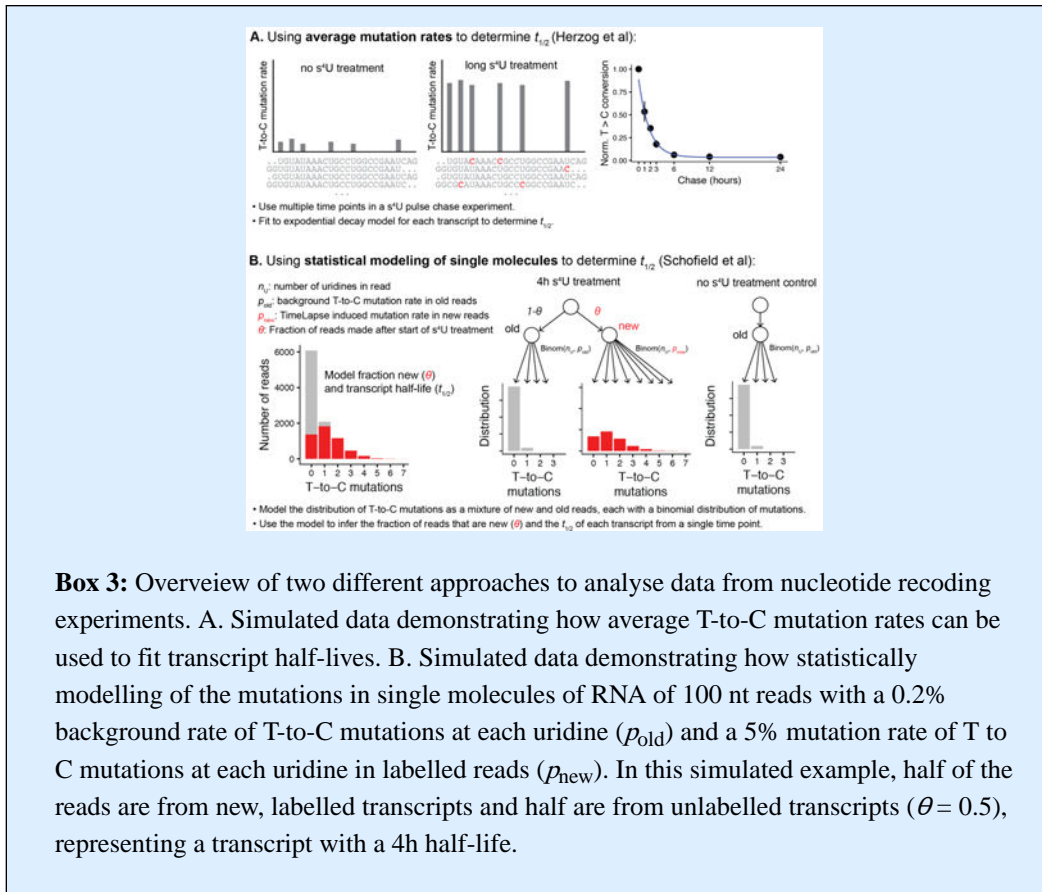
Box 3: Overveiew of two different approaches to analyse data from nucleotide recoding experiments. A. Simulated data demonstrating how average T-to-C mutation rates can be used to fit transcript half-lives. B. Simulated data demonstrating how statistically modelling of the mutations in single molecules of RNA of 100 nt reads with a 0.2% background rate of T-to-C mutations at each uridine (p_{old}) and a 5% mutation rate of T to C mutations at each uridine in labelled reads (p_{new}). In this simulated example, half of the reads are from new, labelled transcripts and half are from unlabelled transcripts ($\theta = 0.5$), representing a transcript with a 4h half-life.
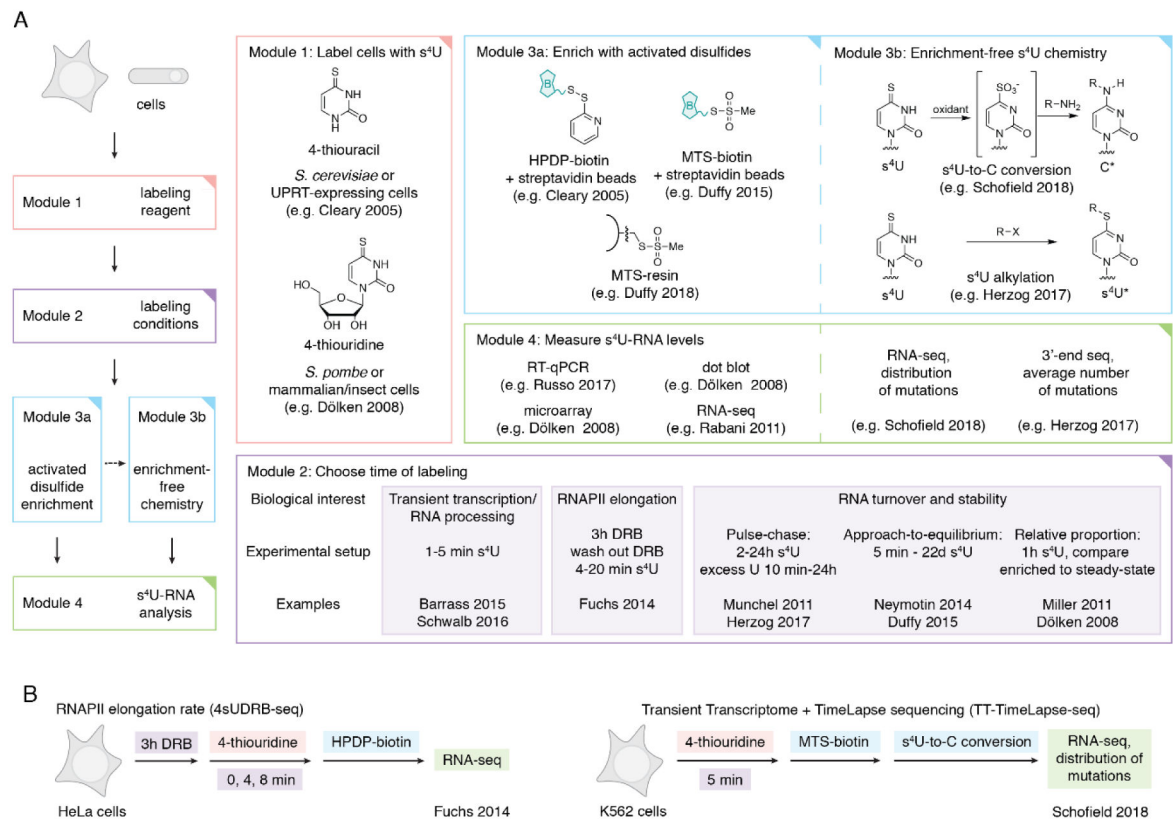
Figure 1:

(A) Overview of s4U metabolic labeling experiments. Different options are indicated for each module, along with references for representative examples. In the case where two references are listed, the first applies to yeast and the second to mammalian cells, as the time of s4U labeling can vary widely between organisms. (B) Representative examples of two s4U metabolic labeling experiments that leverage different module options: 4sUDRB-seq to measure RNAPII elongation and TT-TimeLapse-seq to detect unstable RNAs.
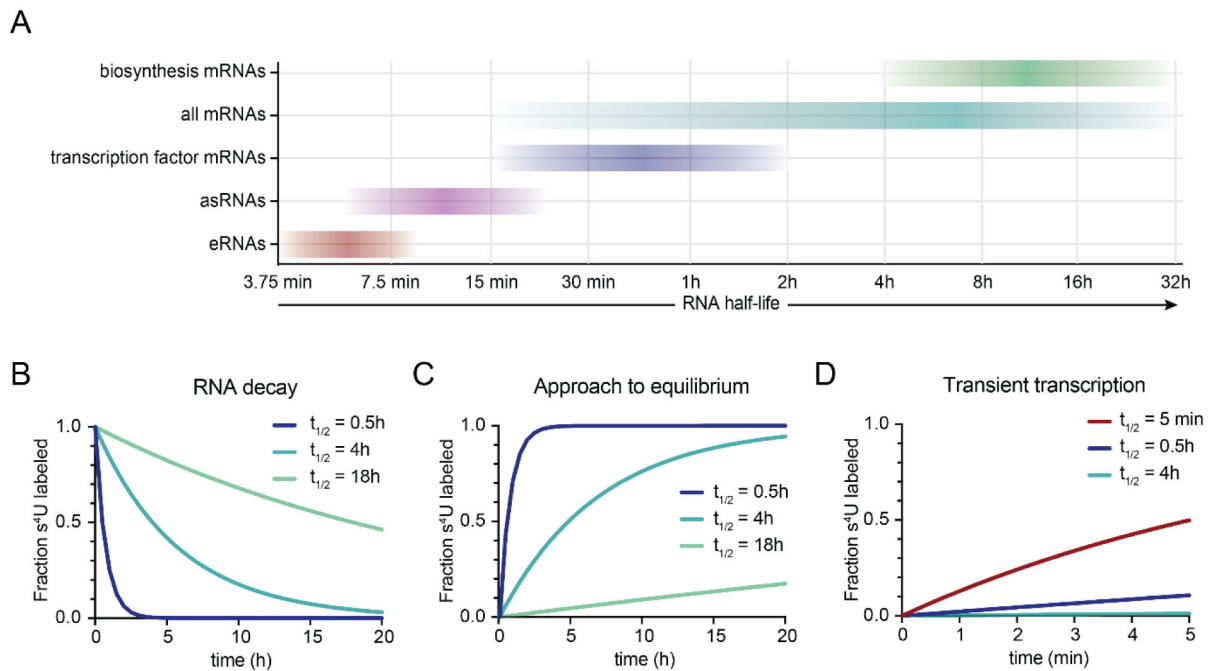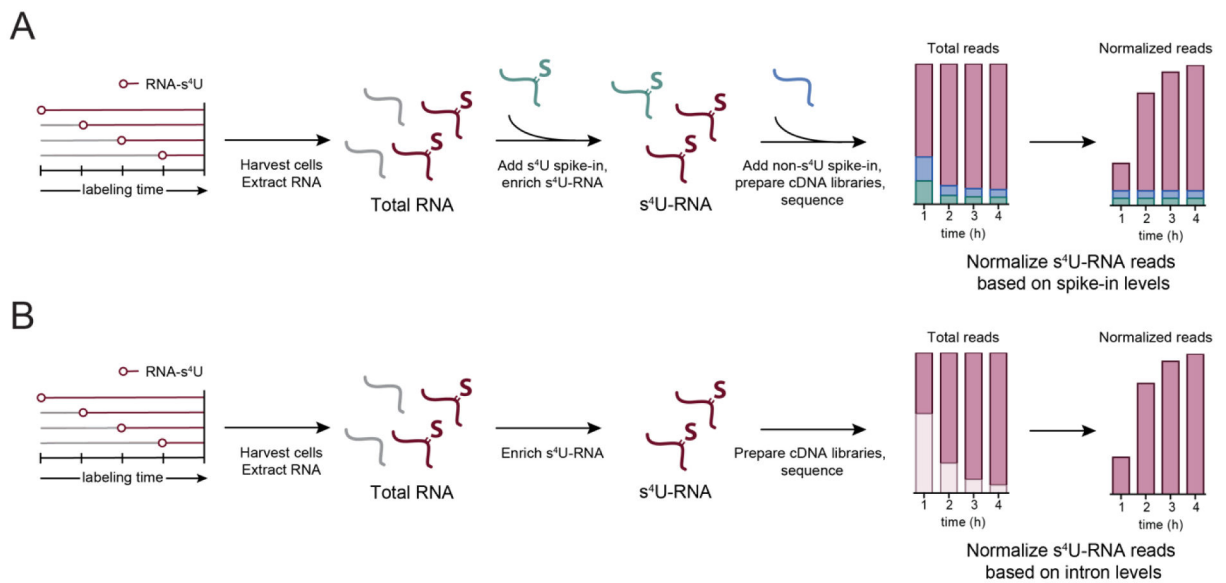
Figure 2:
(A) Estimated range of RNA half-lives in mammalian cells based on data from (Schofield et al., 2018; Schwalb et al., 2016; Yang et al., 2003). (B) Simulation of RNA decay rates for a s^{4}U pulse-chase experiment for three different RNA half-lives, represented as a fraction of the total amount of s^{4}U-labeled RNA at the start of the chase. (C) Simulation of s^{4}U approach-to-equilibrium kinetics for three different RNA half-lives. (D) Kinetics of s^{4}U incorporation during 5 min of s^{4}U labeling for a transient RNA (t$_{1/2}$ = 5 min) and two mRNAs (t$_{1/2}$ = 0.5h and 4h).
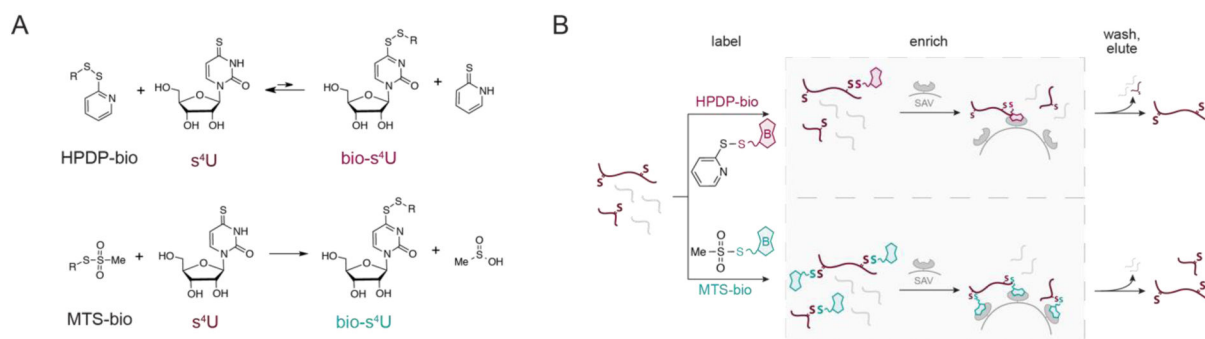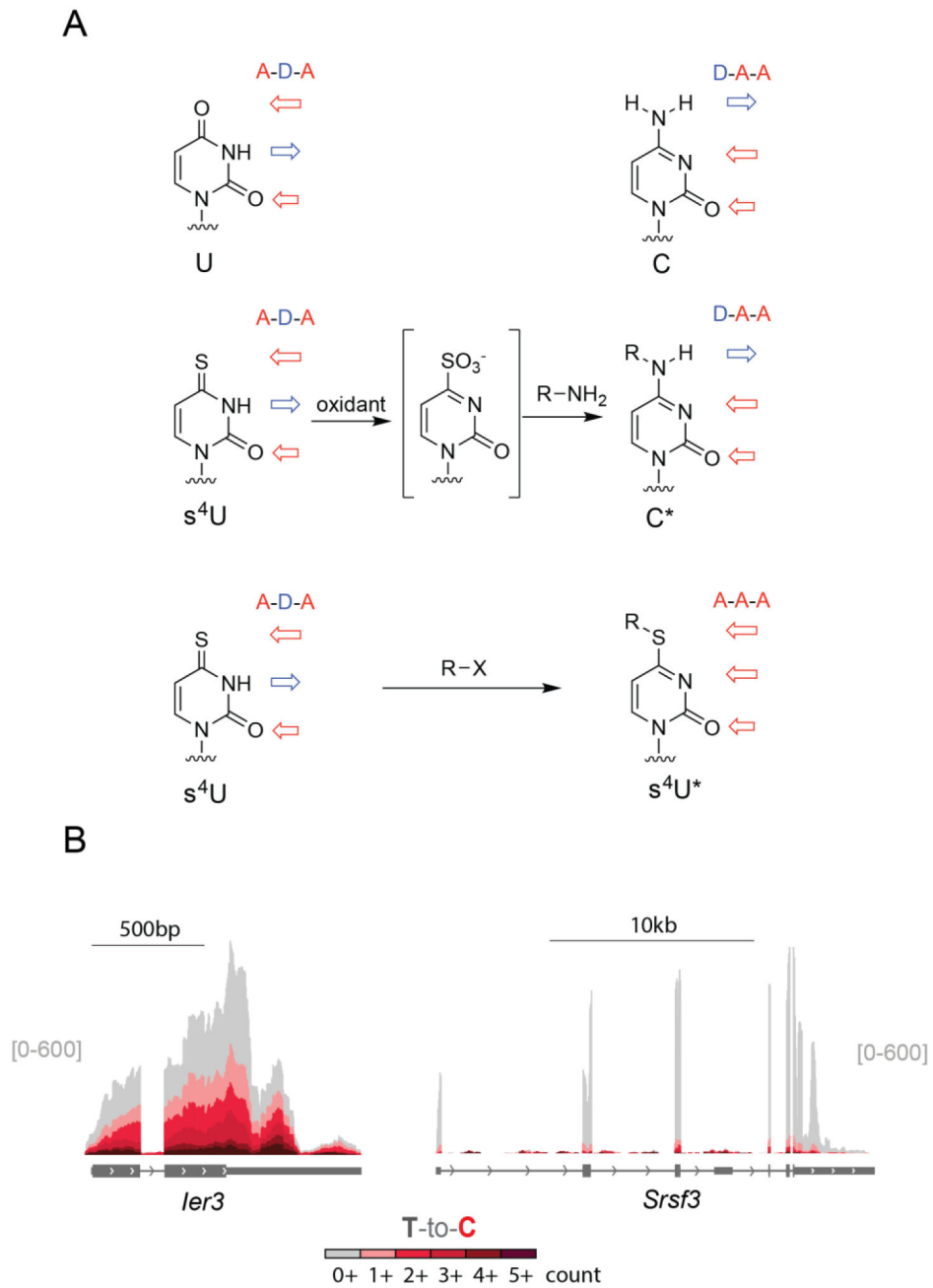
Figure 3:
Significance of inefficient chemistry toward length bias in s⁴U metabolic labeling experiments. (A) Chemistry of activated disulfide reactivity with s^{4}U. When HPDP-biotin is used as the activated disulfide, any biotin-s^{4}U (bio-s^{4}U) product results in a more activated disulfide due to the electron-poor pyrimidine ring of s^{4}U, therefore favoring the reverse rather than the forward biotinylation reaction. In contrast, MTS-biotin reacts irreversibly with s^{4}U to form the bio-s^{4}U product under the reaction conditions, and the covalent disulfide bond can only be reversed under reducing conditions. (B) Schematic of s^{4}U-RNA enrichment with HPDP- and MTS-biotin. Efficient activated disulfide reactivity of MTS-biotin results in greater yields of s^{4}U-RNA and alleviates potential biases toward longer RNAs with more uridines.

Figure 4:

Methods to normalize s^{4}U-RNA data after high-throughput sequencing. (A) After cells are metabolically labeled with s^{4}U and total RNA is extracted, exogenous s^{4}U-RNA (s^{4}U-labeled RNA from *S. pombe*, or *in vitro*-transcribed s^{4}U-RNAs) are added to each sample and then enriched. Alternatively or in addition, exogenous RNA without s^{4}U can also be added to samples after enrichment. Samples are then analyzed by high-throughput sequencing and normalized based on the number of reads that align to the spike-in sample. (B) Samples can also be enriched without RNA spike-ins and normalized based on the relative proportion of introns in each sample (Lugowski et al., 2018). First, intron coverage for each transcript is determined based on the number of reads that map to introns in the longest isoform of a given transcript without overlapping exons or any other isoform. Next, introns are filtered for coverage and time-dependent changes in expression. Reads that map to exons are finally normalized to the sum of all reads mapping to the well-behaved intron set.

Figure 5:

(A) Hydrogen bonding pattern of modified or recoded s4U nucleosides following enrichment-free chemistry. (B) Example TimeLapse-seq tracks adapted from Schofield et al. 2018 for faster turnover (Ier3) and slower turnover (Srsf3) transcripts in MEF cells treated with 1 mM s4U for 1h.

Table 1:

Examples of studies using s^{4}U labeling to assess mRNA stability in cell lines of different organisms.

Human			
Cell type	**Concentration**	**Time of feed**	**Citation**
BL41 (lymphoma)	100 μM s^{4}U	1h	Dölken 2008, Friedel 2009
HeLa (cervical carcinoma)	100 μM s^{4}U 250 μM s^{4}U	1h 1h	Dölken 2008 Borowski 2014
Jurkat (T tymphocyte)	100 μM s^{4}U 200 μM s^{4}U	1h 1h	Dölken 2008 Blackinton 2016
DG75 (B lymphocyte)	100 μM s^{4}U 500 μM s^{4}U	1h 5–60 min	Dölken 2008 Windhanger 2012
HEK293T (embryonic kidney)	250 μM s^{4}U 100 μM s^{4}U 700 μM s^{4}U	1h 20 min-22 d 1h	Borowski 2014 Duffy 2015 Gregersen 2014, Duffy 2015
293A (embryonic kidney	2.5 μM s^{4}U	2h	Stubbs 2015
iPS (stem cell	400 μM s^{4}U	2h	Russo 2017
LCL (lymphoblast)	200 μM s^{4}U	2h	Duan 2013
MEWO (melanoma)	500 μM s^{4}U	1h	Azarkh 2011
Primary T-cells	200 μM s^{4}U	1-6h	Payne 2014
RAJI (lymphoblast)	300 μM s^{4}U	30 min	Donato 2016
RCC (renal carcinoma)	2 μM s^{4}U	2h	Bresson 2015
SH-SY5Y (neuroblastoma)	500 μM s^{4}U	30 min	Schwarzl 2015
143B (osteosarcoma	250 μM s^{4}U	1h	Borowski 2014
K562	500 μM s^{4}U 100 μM s^{4}U 1 mM s^{4}U	5 min 4h 5 min	Schwalb 2016 Schofield 2018 Duffy 2018
MDA-MB-231 (breast cancer)	200 μM s^{4}U	20 min	Cho 2018
MCF7 (breast cancer)	400 μM s^{4}U	2h	Schwanhausser 2011
Mouse			
NIH-3T3 (fibroblasts)	200 μM s^{4}U 500 μM s^{4}U 400 μM s^{4}U	1h <30 min 2h	Dölken 2008 Dölken 2008 Schwanhausser 2011
RAW 264.7 (macrophages)	100 μM s^{4}U	1h	Dölken 2008
SVEC 4–10 (endothelial)	100 μM s^{4}U	1h	Dölken 2008
MEF	1 mM s^{4}U 200 μM s^{4}U	1h 2h	Schofield 2018 Kenzelmann 2007
Primary T-cells	250 μM s^{4}U	15 min	Li 2017
Dendritic cells	150 μM s^{4}U	45 min	Rabani 2011
Yeast			
S. cerevisiae + UPRT	200 μM 4-thiouracil	3h	Muchel 2011

Human

Cell type	Concentration	Time of feed	Citation
S. cerevisiae + hENT1	500 μM s⁴U	3-24 min	Miller 2011
S. cerevisiae *S. pombe*	5 mM 4-thiouracil 500 μM s⁴U	6 min 6 min	Sun 2012 Sun 2012
S. cerevisiae + FUI1	100 μM s⁴U	2-7 min	Swaitkowska 2012
S. cerevisiae	500 μM 4-thiouracil	3-100 min	Neymotin 2014
S. cerevisiae + FUI1	500 μM 4-thiouracil	1.5-5 min	Barrass 2015
S. cerevisiae	50 μM 4-thiouracil	16h	Miller 2018

Other

Cell type	Concentration	Time of feed	Citation
H. volcanii	300 μM 4-thiouracil	45 min	Knüppel 2017
S. acidocaldarius	135 μM 4-thiouracil	45 min	Knüppel 2017
D. melanogaster kc167	500 μM s⁴U	5-20 min	Pai 2017
D. melanogaster kc167	300 μM s⁴U	30-450 min	Chen and van Steensel 2017
D. melanogaster S2	200 μM s⁴U	2-6h	Khong 2017
D. rerio (zebrafish) embryo	1 nL 50 mM s⁴UTP	0-9 cell divisions	Heyn 2014